Published in final edited form as:
Sci Immunol. ; 2(10): . doi:10.1126/sciimmunol.aam9628.

Complement factor P is a ligand for the natural killer cell–activating receptor NKp46

Emilie Narni-Mancinelli[1,*], **Laurent Gauthier**[#2], **Myriam Baratin**[#1], **Sophie Guia**[#1], **Aurore Fenis**[#1], **Ala-Eddine Deghmane**[3], **Benjamin Rossi**[2], **Patrick Fourquet**[1,‡], **Bertrand Escalière**[1], **Yann M. Kerdiles**[1], **Sophie Ugolini**[1], **Muhamed-Kheir Taha**[3], and **Eric Vivier**[1,4,*]

[1]Centre d'Immunologie de Marseille-Luminy, Aix Marseille Université, Inserm, CNRS, Marseille, France

[2]Innate Pharma, Marseille, France

[3]Institut Pasteur, Invasive Bacterial Infections Unit and National Reference Center for Meningococci, Paris, France

[4]Service d'Immunologie, Hôpital de la Timone, Assistance Publique-Hôpitaux de Marseille, Marseille, France

[#] These authors contributed equally to this work.

Abstract

Innate lymphoid cells (ILCs) are involved in immune responses to microbes and various stressed cells, such as tumor cells. They include group 1 [such as natural killer (NK) cells and ILC1], group 2, and group 3 ILCs. Besides their capacity to respond to cytokines, ILCs detect their targets through a series of cell surface–activating receptors recognizing microbial and nonmicrobial ligands. The nature of some of these ligands remains unclear, limiting our understanding of ILC biology. We focused on NKp46, which is highly conserved in mammals and expressed by all mature NK cells and subsets of ILC1 and ILC3. We show here that NKp46 binds to a soluble plasma glycoprotein, the complement factor P (CFP; properdin), the only known positive regulator of the alternative complement pathway. Consistent with the selective predisposition of patients lacking CFP to lethal *Neisseria meningitidis* (Nm) infections, NKp46 and group 1 ILCs bearing this receptor were found to be required for mice to survive Nm infection. Moreover, the beneficial effects of CFP treatment for Nm infection were dependent on NKp46 and group 1 NKp46+ ILCs.

[*]Corresponding author. narni@ciml.univ-mrs.fr (E.N.-M.); vivier@ciml.univ-mrs.fr (E.V.).
[‡]Present address: Marseille Protéomique, CRCM, Institut Paoli-Calmettes, Aix Marseille Université, Inserm, CNRS, Marseille, France

Author contributions: E.N.-M. and E.V. conceived the project. L.G. and M.B. generated and characterized the 27A1.7 mAb and performed proteomic analysis with the help of P.F. A.F. and B.R. generated recombinant soluble molecules. L.G. performed SPR experiments. S.G. designed and performed CRISPR/Cas9 gene silencing. Y.M.K. analyzed ILC depletion after antibody treatment. E.N.-M., M.-K.T., and E.V. designed and analyzed Nm infection studies. M.-K.T., A.-E.D., and S.G. performed Nm infection experiments. B.E. analyzed RNA sequencing data. E.N.-M., L.G., S.U., M.-K.T., and E.V. analyzed data. E.N.-M. and E.V. wrote the manuscript with the help of the other authors.

Competing interests: E.V. is a cofounder of Innate Pharma. E.V. and S.U. are shareholders in Innate Pharma. L.G. and B.R. are employed by Innate Pharma. All other authors declare that they have no competing interests. E.N.-M., L.G., M.B., and E.V. are inventors on the patent (no. 62/417,444) submitted by Inserm Transfert that covers natural ligands of NKp46 and compositions and methods for modulating NK cell activation through NKp46 receptors.

Europe PMC Funders Author Manuscripts

Thus, group 1 NKp46+ ILCs interact with the complement pathway, via NKp46, revealing a cross-talk between two partners of innate immunity in the response to an invasive bacterial infection.

Introduction

Innate lymphoid cells (ILCs) comprise various types of lymphocytes lacking rearranged antigen-specific receptors (1, 2). Natural killer (NK) cells are cytotoxic ILCs that have been originally described as being capable to kill tumor cells without any previous antigen-specific activation. NK cells also participate in the clearance of microbial infection through their cytotoxic properties and cytokine secretion such as the production of interferon-γ (IFN-γ) (3). NK cells can also act as regulatory cells and contribute to shaping adaptive immune responses by acting on macrophages, dendritic cells, and T cells (3).

NK cell effector activities are tightly controlled by a fine balance of inhibitory and activating signals delivered by surface receptors (4, 5). Inhibitory receptors gauge the absence or the decrease in constitutively expressed major histocompatibility complex class I (MHC-I) self-molecules on target cells. A decrease in MHC-I expression reduces the strength of inhibitory signals delivered to NK cells, rendering them more prone to be activated (6–8). NK cell activation results from the engagement of an array of activating receptors, such as the activating isoforms of Ly49 and KIRs (killer cell immunoglobulin-like receptors), the natural cytotoxicity receptors (NCRs), the SLAM (signaling lymphocyte activating molecule)–related receptors, NKG2D, and CD16 (9, 10). The NCR group is composed of three molecules: NKp30 (NCR3, CD337) and NKp44 (NCR2, CD336) in humans and NKp46 (NCR1, CD335), which is highly conserved in mammals (11). NKp46 is mainly expressed by NK cells and ILC1, except for a small population of T lymphocytes and a subset of ILC3 (NCR+ ILC3) in mucosa (12–14).

Activating receptors can recognize two types of ligands: self-molecules whose expression is induced upon cellular stress or exogenous molecules produced by microbes during infections (15, 16). For example, NCRs have been described to bind several but not all hemagglutinin and hemagglutinin neuraminidases of the influenza, Sendai, Newcastle disease, ectromelia, and vaccinia viruses. NKp46 could also recognize PfEMP1 of *Plasmodium falciparum*, an unknown ligand from *Fusobacterium nucleatum*, and adhesins from *Candida glabrata* (16–19). Besides the finding that the cell surface transmembrane protein B7-H6 is a ligand for NKp30 (20) and that the three NCRs can bind to different heparan sulfate sequences (21–23), the identification of nonmicrobial ligands for NCRs remains to be completed (16). Along this line, it has been described that NKp30 recognizes the nucleic factor human leukocyte antigen- B–associated transcript BAT3 that can be expressed in the cytoplasm of tumor and apoptotic cells. Similarly, NKp44 can recognize the proliferating cell nuclear antigen and the mixed-lineage leukemia protein 5–related NKp44L, which are normally expressed in the nucleus of healthy cells but can be found in the cytoplasm of tumors cells (24). NKp46 has been described to bind the intracellular filamentous cytoskeletal protein vimentin expressed on the surface of *Mycobacterium tuberculosis*–infected monocytes (25). Notably, it has been reported that NKp46 could recognize a surface protein on healthy pancreatic β cells (26), but this cellular ligand still

Europe PMC Funders Author Manuscripts

awaits identification. The knowledge of the function of NKp46 is key to understanding the biology of three major ILC subsets. We therefore developed a strategy to identify cellular ligands of NKp46 in the absence of microbial infection.

Results

Identification of NKp46 ligand candidates

We used a high-affinity screening system based on interleukin-2 (IL-2) secretion by a DO11.10 mouse T cell reporter engineered to express a chimeric cell surface receptor consisting of the extracellular domains of either human or mouse NKp46 fused to mouse CD3ζ (HuDOMsp46 and MoDOMsp46 cells, respectively). Using the same strategy, we also generated a DOMsp30 reporter cell expressing the extracytoplasmic domain of NKp30 fused to mouse CD3ζ as a control (20). Sv40 (Simian virus 40)–transformed mouse embryonic B12 fibroblasts expressed a ligand for NKp46 because (i) B12 cells induced IL-2 production by both human and mouse DOMsp46 reporter cells but not by DOMsp30 or parental control DO11.10 cells and (ii) DOMsp46 activation by B12 cells was blocked by anti- NKp46 monoclonal antibodies (mAbs) and reliable NKp46-Fc fusion molecules (Fig. 1, A to C, and fig. S1) but not by anti-NKp30 mAbs and NKp30-Fc or MICA-Fc fusion molecules (fig. S2). We sought to characterize the ligands for NKp46 expressed by B12 tumor cells by generating mAbs against B12 cells and assessing their capacity to interfere with the B12 cell–mediated activation of DOMsp46 cells. The 27A1.7 mAb stained the surface B12 cells and partially blocked DOMsp46 activation by B12 cells, suggesting that it might recognize a ligand for NKp46 (Fig. 1D and fig. S3A). Mass spectrometry revealed the presence of only two molecules in the material immunoabsorbed by 27A1 mAbs: the junctional adhesion molecule JAM1 and the complement factor P (CFP).

CFP binds to NKp46

Surface plasmon resonance (SPR) experiments showed that the binding of B12 cell lysates to a 27A1.7 mAb–coated biosensor was inhibited by anti-JAM1 mAb and that JAM1-Fc bound to the 27A1.7 mAb–coated biosensor, demonstrating the specificity of 27A1.7 mAb for JAM1 (fig. S3, B and C). We thus knocked down JAM1 expression in B12 cells with the clustered regularly interspaced short palindromic repeat/caspase 9 (CRISPR/Cas9) system and showed that this abolished the binding of the 27A1.7 mAb to B12 cells (fig. S3D). We then directly assessed the interaction of JAM1 with NKp46 by SPR (fig. S3E). We observed no direct interaction between JAM1-Fc and NKp46-Fc.

CFP, also known as properdin, is a plasma glycoprotein produced by many different leukocyte subsets, including neutrophils, monocytes, and T cells (27). It is the only positive regulator of the alternative complement pathway identified so far and stabilizes the C3 and C5 convertases (27). We detected binding between serum-purified human CFP and human NKp46-Fc but no binding to the control NKp30-Fc (Fig. 2A) or to the 27A1.7 mAb. These data suggest that 27A1.7 binds to a larger molecular complex containing CFP. This binding could occur via JAM1 if it is part of this molecular complex. Irrespective of this possibility, we next focused on the interaction between CFP and NKp46. We also generated recombinant human and mouse HIS-tagged CFP proteins (fig. S4), and SPR experiments

with various concentrations of recombinant CFP revealed similar patterns of avidity for human and mouse NKp46-Fc, and a lack of binding to NKp30-Fc–coated biosensors (Fig. 2B and table S1). Notably, because native CFP is described to be naturally present in serum as oligomers assembled into dimers (P2), trimers (P3), and tetramers (P4), we confirmed the binding of dimeric and tetrameric purified CFP fractions to NKp46-Fc–coated biosensors (fig. S5). We also performed a flow cytometry assay, in which NCR-Fc molecules were covalently bound to beads and incubated with HIS-tagged CFP proteins (Fig. 2, C to G). We observed cross-species interactions of NKp46-Fc with CFP, as recombinant human CFP bound both human and mouse NKp46-Fc, and mouse CFP bound both human and mouse NKp46-Fc, albeit not to the same extent (Fig. 2, C to E). These results are consistent with the strong conservation of both NKp46 and CFP across mammals, with high levels of identity (62% for NKp46 and 77% for CFP) for their amino acid sequences between humans and mice. The NKp30-Fc control molecule did not interact with CFP in this assay. A dose-dependent response was observed for CFP binding to NKp46 over the physiological range of CFP concentrations (5 to 50 μg/ml) (Fig. 2F). The CFP-NKp46 interaction was inhibited by anti-NKp46 blocking mAbs (Fig. 2G). Thus, serum-purified and recombinant CFP can bind to recombinant NKp46-Fc fusion molecules. Using the available tools, we were unable to detect the surface expression of CFP or soluble CFP released from B12 cells. Nevertheless, we assessed and observed *Cfp* mRNA expression in B12 cells by reverse transcription quantitative polymerase chain reaction (PCR) through comparisons with two other embryonic mouse fibroblast cell lines: 2sv and NIH-3T3 (fig. S6A). In addition, polyclonal antibodies (pAbs) against CFP partially blocked NKp46 reporter cell activation against B12 cells (fig. S6B). CRISPR/Cas9-mediated silencing of *Cfp* in B12 cells resulted in the mutated B12 cells being unable to activate DOMsp46 reporters (Fig. 3), completing our demonstration of CFP acting as a ligand for NKp46.

CFP binds to NKp46-expressing cells

We then assessed the binding of recombinant CFP to cell surface NKp46. We found that CFP bound to human and mouse NKp46-expressing DOMsp cells (HuDOMsp46 and MoDOMsp46 cells) but not to DOMsp cells expressing NKp30 (DOMsp30 cells) (Fig. 4A). CFP also bound to human KHYG1-NKp46 NK cells genetically modified to express large amounts of NKp46 but not to the parental KHYG1 cells, which express only small amounts of NKp46 (Fig. 4B). In addition, we detected the binding of CFP to human IL-2–activated NKp46+ bulk NK cells but not to T cells present in the same cell preparations (Fig. 4C and fig. S7). Thus, both primary NKp46+ cells and cells engineered to express NKp46 bind soluble CFP.

CFP does not induce classical NK cell activation

Prototypical NK cell–activating receptors, such as NKG2D and NKp30, trigger NK cells when they bind to their ligands (28). By contrast, we could not detect NK cell activation after CFP stimulation, as assessed by measuring the expression of CD107, as a marker of cell degranulation, or IFN-γ secretion (fig. S8). Using RNA sequencing, we observed up-regulation of *Ifng* and *Ccl3* transcripts in freshly isolated NK cells stimulated with anti-NKp46 mAbs, as expected, but not with CFP (Fig. 5A). The only genes up-regulated upon both anti-NKp46 and CFP stimulations were *Fosb* encoding a leucine zipper protein and

Xcl1 encoding the lymphotactin chemokine (Fig. 5A and tables S2 and S3). Global analysis revealed a stimulation of several pathways involved in cell metabolism, signal transduction, transport, and transcription upon anti-NKp46 mAb treatment (Fig. 5B and table S2), as expected. A very different pattern of regulation was observed upon CFP treatment (Fig. 5 and table S3), with several pathways being down-regulated in this condition. Therefore, CFP acts as a ligand for NKp46 but initiates a transduction pathway on NK cells, which is distinct from the canonical pathway induced by anti-NKp46 mAbs.

NKp46$^+$ ILCs and NKp46 are required for mouse survival to Neisseria meningitidis invasive bacterial infection

CFP deficiency is associated almost exclusively with severe *Neisseria meningitidis* (Nm) infections in humans, highlighting the key role of this molecule in defense against such infections (29). Nm is a Gram-negative, aerobic, encapsulated diplococcus that causes invasive meningococcal disease, with meningitis and septicemia, an emerging public health problem (30–32). Numerous Nm serogroups have been defined on the basis of their capsular polysaccharide antigens, including six (A, B, C, W135, X, and Y) that can cause epidemics. We investigated the biological relevance of CFP-NKp46 interaction in vivo during invasive Nm infection in mice using the serogroup B MC58 strain. We assessed the requirement of NKp46$^+$ cells for survival upon Nm infection using *Ncr1*-iCre mice crossed with *R26*$^{lslDTA/+}$ mice, which are essentially devoid of NKp46$^+$ cells (33). Mice without NKp46$^+$ cells were more susceptible to Nm infection than their control littermates and were less able to clear bloodborne Nm (Fig. 6, A and B). NKp46+ cells include NK cells, subsets of ILC1, and NCR$^+$ ILC3 (12). The treatment of mice with anti-NK1.1 mAbs led to the efficient in vivo depletion of NK cells and ILC1 but had little impact on NCR$^+$ ILC3 (fig. S9). NK1.1-depleted mice had higher mortality rates than the control group (Fig. 6C) and 8 to 20 times more bacteria in their blood (Fig. 6D). These results show that group 1 ILCs (i.e., NK cells and/or NKp46$^+$ ILC1) are involved in controlling Nm infection in mice. No tools are currently available for the specific depletion of NK cells or ILC1. Nevertheless, we also treated mice with depleting aGM1 antibodies, which target NK cells more strongly than ILC1s (fig. S9) (34); this treatment resulted in an increase in Nm bacteremia similar to that seen with anti-NK1.1 mAbs (fig. S10), suggesting that NK cells might be the primary group 1 NKp46$^+$ cell type involved in controlling Nm infection in this mouse model.

NKp46 recognizes serum-opsonized Nm and is required for mice survival to Nm infection

We then investigated whether NKp46 itself was involved in the mechanisms controlling Nm infection. NKp46-deficient mice were more susceptible to Nm infection than their control littermates after the delivery of moderate doses of inoculum, and they died significantly sooner after challenge with high doses of Nm (Fig. 6E). The lack of Nm control was associated with higher bacterial load in the blood of *Ncr1*$^{GFP/GFP}$ mice than in control mice (Fig. 6F). These results demonstrate the dependence on NKp46 expression for the protective immunity during Nm infection.

We further dissected the mechanisms involved in this NKp46-dependent pathway controlling Nm infection by investigating whether NKp46 could bind Nm. Soluble NKp46-Fc proteins did not directly bind to Nm bacteria, similarly to NKp30-Fc (Fig. 7A). Because Nm is an

extracellular bacterium targeted by CFP in vivo, we assessed the binding of NKp46-Fc proteins on Nm opsonized by CFP using serum. We detected NKp46-Fc binding on serum-opsonized Nm but not with control NKp30-Fc molecules (Fig. 7A). This binding signal was lost if the bacteria were opsonized with CFP-depleted serum (Fig. 7, B and C). These results suggest that NKp46 confers to group 1 ILCs the possibility to interact with Nm via CFP. Together with the critical role of CFP in defense against Nm, these data are consistent with a role for interaction between NKp46 and CFP in the control of this invasive bacterial infection by NKp46$^+$ ILCs.

Primary NKp46$^+$ ILCs participate in the therapeutic benefit of CFP delivery for Nm bacterial control in vivo

We thus investigated whether NKp46$^+$ ILCs and NKp46 were required for the protective role of CFP during Nm infection. As shown previously (35), treatment with exogenous CFP protected wild-type (WT) mice from Nm infection, where bacteremia was 16 and 84% lower in CFP-treated mice than in the untreated group 24 and 48 hours after infection, respectively (Fig. 8, A to D). By contrast, CFP treatment failed to induce Nm clearance from the blood in surviving anti-NK1.1 mAb–treated mice (Fig. 8, B to D). Moreover, the CFP treatment of *Ncr1GFP/GFP* NKp46–deficient mice resulted in a much reduced clearance of bacteria from the blood than for the control group (4 and 28% versus 49 and 100% at 24 and 48 hours after infection, respectively) (Fig. 8, E to H). Indeed, NKp46-deficient mice still presented septicemia 48 hours after infection. Nevertheless, CFP delivery in this setting was sufficient to rescue NKp46-deficient mice from death (fig. S11), showing that there are NKp46-independent functions of CFP, a finding that is not unexpected. Nonetheless, the therapeutic effects of recombinant CFP delivery for decreasing Nm bacteremia were dependent on NKp46 and NKp46$^+$ ILCs.

Discussion

We have shown here that CFP is a ligand for the NCR NKp46. Consistent with this finding, NKp46 was critical during meningococcal infection, a disease in which CFP is required for survival. The high incidence of fulminant Nm infections characteristic of CFP-deficient patients contrasts with the lack of mortality in patients with late complement pathway defects [i.e., membrane attack complex (MAC) deficiencies] (36). These results suggest that control of Nm infection depends on CFP and not on MAC. The CFP- and NKp46-dependent pathway responsible for controlling Nm infection, which we revealed here, may be involved in this MAC-independent function of CFP during Nm infections.

Our data showed that CFP binds to NKp46. Nevertheless, several results remained unexplained. During our screening assay, we were able to detect NKp46 reporter cell activation only when cocultured with B12 cells but not with mycoplasma-free cell lines previously described as expressing an NKp46 ligand, such as the mouse lymphoma YAC-1, the mouse thymoma BW1502, the human melanoma M14, or the EBV-transformed human B cell line (37). We did not detect CFP staining at the surface of B12 cells, but *Cfp* gene silencing abrogated NKp46 reporter cell activation. Last, CFP stimulation did not induce the canonical NK cell activation pathway as compared with anti-NKp46 mAb stimulation that

induces, for instance, IFN-γ and CCL3 secretion. However, both anti-NKp46 mAbs and CFP stimulations of NK cells lead to the up-regulation of the transcripts encoding the chemokine *Xcl1*. Beside its role as a ligand for the XCR1 receptor associated with dendritic cells mediating antigen cross-presentation (38), XCL1 exhibits a broad-spectrum antibacterial activity by causing bacterial membrane disruption in vitro (39, 40). Thus, the importance of XCL1 production and the protective NKp46$^+$ ILCs effector functions during Nm infection need further investigations.

The absence of NK cell activation upon treatment with purified recombinant CFP in vitro also suggests that the interaction of CFP with NKp46 may require additional signals to trigger NKp46$^+$ ILC activation. This possibility is supported by the requirement of NKp46 coengagement with other activating receptors, such as NKG2D, 2B4 (CD244), DNAM-1 (CD226), or CD2 to induce full NK cell activation (41). Along this line, by stimulating the C3 convertase activity, CFP leads to the formation of iC3b, which can interact with both CR3 (CD11b/CD18; expressed on both NK cells and ILC1s) and CR4 (CD11c/CD18; expressed on NK cells). Similar to the requirement of MD2 for signal transduction downstream of the interaction between lipopolysaccharide and Toll-like receptor 4 (42), heparan sulfate glycosaminoglycans (GAGs) may also participate in a CFP-containing molecular complex that could activate NK cells via NKp46 because GAGs have been shown to interact with both NKp46 (43) and CFP (44). Furthermore, it is notable that NKp46 has been shown to physically interact with CD59, an inhibitor of the MAC (45). Thus, our results encourage investigating the interactions between the complement pathway and the biology of group 1 ILCs.

In addition to its role in controlling Nm infection, it has been reported that CFP can also act as a soluble pattern recognition molecule that binds to several other pathogens and apoptotic and necrotic stressed cells (46). These interactions, which remain to be defined molecularly, have been proposed to confer to CFP the possibility to contribute to the elimination of target cells not only by complement activation but also by acting as an opsonin promoting target cell clearance by phagocytes in the absence of complement activation (46). Together with our data, these findings suggest that CFP might contribute to the detection of an array of microbes and cells in distress by ILCs via NKp46. There are also multiple conditions in which CFP participates in host defense, in inflammatory disorders, and in autoimmune diseases, although the molecular underlying mechanisms remain unknown (46). Studies characterizing the cross-talk between NKp46$^+$ ILCs and CFP are therefore of broader interest, extending beyond immunity to Nm infection. Notably, NK cell lymphopenia is associated with increased incidence of invasive bacterial infections and granulomas in patients with common variable immunodeficiency (47). It also remains to be determined whether the reported binding of NKp46 to multiple ligands, including several microbial components (19), involves CFP, which is present in serum and has a propensity to interact with various microbial products. In conclusion, this report shows that CFP binds to human and mouse NKp46 and that NKp46$^+$ group 1 ILCs are required for mice to survive Nm infection, a disease to which CFP-deficient patients are highly susceptible.

Europe PMC Funders Author Manuscripts

Material and Methods

Study design

In most experimental designs, we wanted to compare two (or more) genotypes (first factor) at different time points or under different conditions (second factor). A two-way analysis of variance (ANOVA) was thus the most appropriate analysis method. However, because the genotype effect term was the one of interest, sample estimation was done on the basis of one-way ANOVA. Sample size estimation hypotheses were as follows: two levels for genotype factor, significance level of 5%, power of 80%, and effect size to demonstrate of 1. With these hypotheses, 5.09 mice were needed by genotype and condition (time point or other).

In other experimental designs, we wanted to compare two (or more) groups. A one-way ANOVA was thus the most appropriate analysis method. Sample size estimation hypotheses were as follows: two levels for genotype factor, significance level of 5%, power of 80%, and effect size to demonstrate of 1. With these hypotheses, 5.09 mice were needed.

The data meet the assumptions of the tests except for Fig. 6 (D and H) at 48 hours, so we applied a nonparametric Mann-Whitney test. Except also for Fig. 1D, we applied a nonparametric one-way ANOVA, that is, Kruskal-Wallis test followed by Dunn's multiple comparisons. Variances were similar according to the Brown-Forsythe test and Bartlett test. Statistical significance was determined by oneway ANOVA followed by Dunn's test and two-way ANOVA with Bonferroni or Dunnett correction, as indicated. Unpaired *t* test was performed in fig. S6. Kaplan-Meier curves were used to analyze mouse survival. Significance was calculated by a dose-stratified log rank test. No randomization was performed. No blinding was performed. However, age- and sex-matched litters were used as controls and indicated as such in the figure legends. All animals and samples were included and shown in the figures, as mentioned in the figure legends. No outlier was excluded.

DOMs screening system

The DOMsp30 and DOMsp46 reporter cell lines were generated in a previous study (48). The MoDOMsp46 cells used here were generated in a similar manner. Binding to the chimeric proteins at the surface of these cells triggers IL-2 secretion. We incubated 30,000 cells per well in 96-well plates with tumor targets [effector/target (E:T) ratio of 1:1 to 1:3]. After 20 hours of incubation, we assessed the levels of mouse IL-2 in the cell supernatant, in a standard CTLL-2 survival assay (CellTiter-Glo Luminescent Cell Viability Assay, Promega). S. Jonjic (University of Rijeka) provided the B12 cells. A. Moretta (University of Genoa) provided anti-HuNKp46 BAB281 mAb hybridoma. W. Song (University of Pennsylvania) provided anti-MoCFP pAbs. All cell lines were mycoplasma-free.

NCR-Fc and CFP-HIS fusion proteins

For NCR-Fc fusion proteins, the sequences encoding the extracellular portion of the mouse NKp46 (accession no. A0A0R4IZY7;amino acid 17Q-255N), human NKp46 (accession no. O76036;amino acid 22Q-255N), and NKp30 (accession no. O14931; amino acid 19L-138T) proteins were amplified by PCR from complementary DNA (cDNA) isolated from mouse

and human NK cells. The sequence encoding the Fc portion of human immunoglobulin G1 (IgG1) containing a single substitution (N297Q) was amplified by PCR from cDNA from a designed construction vector. The N297Q mutation prevents the binding of Fc to Fc receptors. For CFP-HIS fusion proteins, the sequences encoding mouse (accession no. P11680; amino acid 24D-464L) and human (accession no. P27918; amino acid 28D-469L) CFP were amplified by PCR from cDNA isolated from mouse splenocytes and human peripheral blood mononuclear cells, respectively. The HIS tag sequence was inserted directly into the reverse primers. PCR-generated fragments were inserted into a mammalian expression vector. Sequencing of the constructs revealed that the cDNAs of all immunoglobulin fusion proteins were in frame with the human Fc genomic DNA and identical to the reported sequences. Similar results were obtained for recombinant HIS-tagged CFP proteins. Chinese hamster ovary (CHO) cells were then stably nucleofected, according to the kit manufacturer's instructions (Amaxa SF Cell Line 4D-Nucleofector X Kit S, Lonza), with the vectors containing the MoNKp46-Fc, HuNKp46-Fc, NKp30-Fc, MoCFP-HIS, or HuCFP-HIS cDNAs. Bulk CHO cells were then subcloned. Each selected subclone was cultured in serum-free CD CHO complete medium (Gibco) for 8 days, and supernatants were collected. NCR-Fc proteins were purified with Protein A Sepharose Fast Flow (GE Healthcare Life Sciences), and HIS-tagged CFP proteins were purified on Ni-NTA agarose (Qiagen). Proteins were then separated by size exclusion chromatography on a Superdex 200 Increase 10/300 GL column coupled to an ultraviolet (UV) detector (Akta Pure 3, GE Healthcare). All these tools were generated at Innate Pharma. Quality controls are presented in figs. S1 and S2.

Generation of mAbs against B12 cells

Briefly, plasmocytes from rats immunized with 15×10^6 B12 cells (provided by S. Jonjic) were fused with myeloma X63 by standard methods at the mAb platform of the Centre d'Immunologie de Marseille-Luminy (CIML). After standard selection on aminopterin for 15 days, hybridomas were screened by fluorescence-activated cell sorting (FACS) for the positive surface staining of B12 cells and the negative staining of DO11.10 cells. We investigated the ability of nine selected hybridomas to inhibit HuDOMsp46 activation in coculture with B12 cells. Specific inhibition was observed only for the 27A1.7 mAb.

Identification of candidate NKp46 ligands

Lysates from 5×10^8 B12 cells and control serum were subjected to immunoprecipitation with the 27A1.7 mAb or rat IgG2b. The column was washed twice with HBS-EP buffer [10 mM Hepes (pH 7.4), 150 mM NaCl, 3 mM EDTA, and 0.005% Tween 20], and the immunoprecipitates were eluted in 10 mM NaOH and 500 mM NaCl. The various fractions were subjected to SDS–polyacrylamide gel electrophoresis, and the gels were stained with Imperial Protein Stain. The bands were excised and further analyzed by the CIML Proteomics Platform. Proteins were reduced by incubation with 100 mM dithiothreitol for 45 min at 56°C, and free cysteine residues were capped by incubation with 100 mM iodoacetamide for 30 hours at 25°C in the dark. Samples were digested with porcine trypsin (V5111, Promega) at a concentration of 12.5 ng/μl in 25 mM NH4HCO3 for 18 hours at 37°C. Peptides were extracted from the gel with 60% (v/v) acetonitrile in 5% formic acid, dried under vacuum, and reconstituted in 5 μl of 50% (v/v) acetonitrile in 0.3%

trifluoroacetic acid. Mass spectrometric analyses were performed on a MALDI-TOF/TOF Bruker Ultraflex III spectrometer (Bruker Daltonics, Wissembourg, France) under the control of the flexControl 3.0 package (Build 51). This instrument was used at a maximum accelerating potential of 25 kV and was operated in reflectron mode and a mass/charge ratio range from 600 to 3700 (RP Proteomics_2015 method). The laser frequency was fixed at 200 Hz, and about 500 shots were accumulated per sample. Five external standards (Peptide Calibration Standard, Bruker Daltonics) were used to calibrate each spectrum to a mass accuracy within 50 ppm. Peaks were selected with flexAnalysis 3.0 software (Bruker) using an appropriate analysis method. The following parameters were used: SNAP peak detection algorithm, S/N threshold fixed to 6, and a quality factor threshold of 30. We mixed 1 μl of sample with 1 μl of a saturated α-cyano-4-hydroxycinnamic acid solution in acetonitrile/0.3% trifluoroacetic acid (1:1). We spotted 1 μl of this mixture onto the target, which was then allowed to dry before analysis by the previously described RP Proteomics_2015 method.

SPR experiments

SPR measurements were performed on a Biacore T100 apparatus (Biacore GE Healthcare) at 25°C. In all Biacore experiments, HBSEP+ (Biacore GE Healthcare) was used as the running buffer, and 10 mM NaOH and 500 mM NaCl were used as the regeneration buffer. Sensorgrams were analyzed with Biacore T100 Evaluation software. We used JAM1-Fc (R&D Systems) human HIS-tagged CFP or CFP purified from serum (TECOmedical-Quidel), as indicated. The recombinant human NKp46-Fc, mouse NKp46-Fc, and human NKp30-Fc proteins were immobilized covalently to carboxyl groups at the surface of C1 Sensor Chips (GE Healthcare). The chip surface was activated with 1-ethyl-3-(3-dimethylaminopropyl) carbodiimide (EDC)/*N*-hydroxysuccinimide (NHS) (Biacore GE Healthcare). Recombinant proteins were diluted to 10 μg/ml in coupling buffer (10 mM acetate, pH 5.2) and injected until the appropriate level of immobilization was achieved (i.e., 700 to 900 response units). The remaining activated groups were deactivated with 100 mM ethanolamine (pH 8) (Biacore GE Healthcare). Binding studies were performed with the classical kinetic wizard (as recommended by the manufacturer). Serial dilutions of soluble analytes (recombinant CFP), ranging from 9 to 600 nM, were injected over the NKp46-Fc–immobilized proteins and allowed to dissociate for 10 min before regeneration. In all experiments, EDC/NHS-activated and ethanolamine-deactivated flow cell 1 served as the reference for blank subtraction.

Cfp and F11r (JAM1) CRISPR editing in B12 cells

We constructed CRISPR plasmids by inserting specially designed guide RNA (gRNA) oligomers into pSpCas9(BB)-2A-GFP plasmids (PX458; a gift from F. Zhang), according to the Zhang laboratory protocol (Addgene plasmid 48138). The following primers were used to construct the gRNA: gRNA Cfp72fwd, caccGTGGCCTCTGTCAGGCATGC; gRNA Cfp72rev, aaacGCATGCCTGACAGAGGCCAC (targeting exon 2 of the *Cfp* gene, chromosome X); gRNA F11r5fwd, caccGTTGGTACAAGGCAAGGGTT; and gRNA F11r-5rev, aaacAACCCTTGCCTTGTACCAAC (targeting exon 2 of the *F11r* gene coding JAM1, chromosome 1). All the oligomers used for this study were synthesized by Sigma-Aldrich. The indicated primer sequences were designed with the e-CRISPR design tool

(www.e-crisp.org/E-CRISP/designcrispr.html). B12 cells were used to seed six well plates at a density of 2×10^5 cells per well. The plates were incubated overnight, and 1×10^6 cells were transfected with 2 μg of PX458-Cfp for nucleofection (NIH/3T3 Cell Line Nucleofector Kit R, program U-030, Lonza) according to the manufacturer's protocol. Two days after transfection, green fluorescent protein (GFP)–positive B12 cells were sorted and cloned with a FACSAria IIIu sorter. The JAM1 mutant clones were screened by expression of JAMA/CD321 (clone H202-106, AbD Serotec) by flow cytometry. For CFP-knockout screening, genomic DNA for the clones was isolated from cells with the DNeasy Blood and Tissue Kit (Qiagen), according to the manufacturer's protocol, and used for PCR analysis. For the detection of genomic deletions, genomic DNA was subjected to PCR analysis with the Taq Platinum High-Fidelity DNA Polymerase (Life Technologies) and appropriate primers. PCR products were purified on a Wizard SV Gel with the PCR Clean-Up System (Promega) and were sequenced, with the appropriate primers, by Eurofins Genomics. CFP protein knockdown was confirmed by inserting the WT cDNA and mutant cDNA in frame with a C-terminal M2 TAG in a eukaryote expression vector. This construct was used to transfect 293T Expi cells, and the cell supernatant and cell lysate were then subjected to Western blotting with an anti–M2-HRP mAb (ab49763, Abcam).

Isolation of CFP oligomers

Pure, frozen recombinant HuCFP-HIS was thawed, and the monomeric, dimeric, trimeric, and tetrameric forms were separated by gel filtration. Briefly, 500 μg of CFP was separated by size exclusion chromatography on a Superdex 200 Increase 10/300 GL column coupled to a UV detector (Akta Pure 3, GE Healthcare). The thawed CFP sample in phosphate-buffered saline (PBS) was loaded onto the column and eluted at a flow rate of 0.75 ml/min.

Flow cytometry measurement of the binding of HIS-tagged CFP to NKp46-Fc

We coupled 10-μm sulfate latex beads (Invitrogen) to protein A-A488 (Molecular Probes) by incubating these two elements together in PBS containing Ca2+Mg2+ for 2 hours. The beads were thoroughly washed and incubated with 2% bovine serum albumin (BSA) in PBS for 1 hour. They were then incubated overnight with NCR-Fc (20 μg/ml) in 2% BSA in PBS. The beads were thoroughly washed, and NCR-Fc was covalently coupled to protein A by incubation with microbial transglutaminase (6 U/ml; Zedira) for 1 hour at 37°C, as previously described (49). Beads were then washed and incubated with the indicated amounts of HIS-tagged CFP protein in veronal buffer (Lonza) and 0.06 M NaCl (pH 7.5) at 37°C for 1 hour in 96-well V-bottomed plates. Where indicated, anti-HuNKp46 mAb (BAB281) or isotype control was added. The beads were washed and treated with 1% paraformaldehyde for 15 min. They were then incubated with biotinylated anti-HIS Tag mAb (5 μg/ml; clone AD1.1.10, R&D Systems) for 30 min at 37°C. The beads were washed, and CFP-HIS/NCR-Fc–coupled beads were detected with a streptavidin-allophycocyanin (APC) (BioLegend). Samples were run on a Canto II cytometry analyzer (BD Biosciences). HIS-tagged CFP was bound directly to beads using anti-mouse beads that were first incubated with a mouse anti-HIS antibody (AD1.1.10) and then with HIS-tagged CFP proteins. Binding was detected with an anti-CFP antibody (fluorescein isothiocyanate, LSBio).

CFP binding to NKp46^{+} cells

We incubated HIS-tagged CFP proteins (10 μg/ml) with biotinylated anti-HIS Tag mAb (5 μg/ml; clone AD1.1.10, R&D Systems) in PBS for 30 min at room temperature. We used 50 μl per sample to stain the following cells: HuDOMsp46, MoDOMsp46, DOMsp30, KHYG1, and KHYG1 Cl3C4 NKp46high cells (Innate Pharma). Cells were incubated for 1 hour at 37°C, washed, and fixed by incubation for 15 min with 1% paraformaldehyde. CFP binding was detected with streptavidin-APC (BioLegend), and NKp46 was detected with anti-NKp46 mAbs (anti-mouse 29A1.7 from eBioscience; anti-human 9E2 from BioLegend). For HIS-tagged CFP binding to primary cells, human IL-2–activated bulk NK and a preparation enriched in mouse NK cells with the NK Cell Isolation Kit II (Miltenyi Biotec) were incubated with precomplexed CFP-HIS/anti-HIS mAb, as described above. Cells were fixed and stained with antibodies against CD56 (V450, BD Biosciences), NKp46 (PE, Beckman Coulter), and CD3 (AmCyan, BD Biosciences) and a dead cell marker (Life Technologies) for human cells. Samples were run on a Canto II cytometry analyzer (BD Biosciences). Cells of interest were gated as live cells (cell lines) or live CD56+CD3−, as indicated in the figure.

CFP stimulation of mouse NK cells

A mouse cell preparation was enriched in NK cells with the NK Cell Isolation Kit II (Miltenyi Biotec) and used directly (resting cells) or cultured with 5000 U of IL-2 (Proleukin, Chiron) for 5 days. Immulon 2HB plates were coated with anti-HIS mAb (AD1.1.10, R&D Systems) or with antibodies against NKp46 (29A1.7, BioLegend) or NKG2D (CX5, eBioscience). When cells were stimulated with HIS-tagged CFP, the plates were coated with anti-HIS mAb at 25 μg/ml and were washed, and the HIS-tagged CFP was then added at a concentration of 100 μg/ml. When indicated, we added IL-12 (2 ng/ml; eBioscience) and IL-18 (5 ng/ml; MBL) or YAC-1 tumor cells (E:T ratio, 1:1). When cells were costimulated with anti-NKp46 or anti-NKG2D antibodies, the plates were coated with mAbs at a concentration of 10 μg/ml. Cells were incubated for 4 hours in the presence of monensin and brefeldin, surface-stained, and then processed for the detection of intracellular IFN-γ. When indicated (fig. S7C), enriched NK cell preparations were incubated overnight with IL-15 (15 ng/ml; PeproTech), with or without soluble HIS-tagged MoCFP (100 μg/ml). Cells in Immulon 2HB plates were then stimulated with IL-12 (2 ng/ml) and IL-18 (5 ng/ml) and coated with anti-NK1.1 antibody (1 μg/ml; eBioscience), anti-Ly49D antibody (3 μg/ml; 4E5, BD Pharmingen), or anti-NKG2D antibody (5 μg/ml). Cells were then incubated for 4 hours in the presence of monensin and brefeldin, surface-stained, and processed for intracellular IFN-γ detection. Gating strategy: live NK1.1+ CD3− NK cells.

RNA sequencing and analysis

A mouse cell preparation was enriched in NK cells with the NK Cell Isolation Kit II (Miltenyi Biotec) and FACS-sorted. Immulon 2HB plates were coated with anti-HIS mAb (AD1.1.10, R&D Systems) or with antibodies against NKp46 (29A1.7, BioLegend) or isotype control rat IgG2a (BioLegend). When cells were stimulated with HIS-tagged CFP, the plates were coated with anti-HIS mAb at 25 μg/ml and were washed, and the HIS-tagged CFP was then added at a concentration of 100 μg/ml. Pure NK cells (500,000) were added per well, and cells were incubated for 4 hours in the presence of monensin and brefeldin.

Europe PMC Funders Author Manuscripts

Cells were lysed in RLT buffer (Qiagen). HalioDx (Marseille, France) processed the samples and performed the RNA sequencing on a NextSeq 500. Bioinformatics was performed by the CIML platform.

Mice, experimental infection, and assessment

Ncr1$^{iCre/+}$*R26*$^{lslDTA/+}$ mice, *NCR1*$^{GFP/GFP}$ mice (provided by O. Mandelboim), and control littermates were bred and maintained under specific pathogen–free conditions at the Centre d'Immunophénomique (Ciphe), Marseilles. C57BL/6 mice were purchased from Janvier Labs. One male LOU/c rat (Harlan) was used to generate mAbs against B12 cells. Infection experiments were conducted at the Pasteur Institute and at the Ciphe. We used 6- to 12-week old male and female mice for the experiments. Mice were maintained under specific pathogen–free conditions, and all experiments were performed in accordance with the rules laid down by institutional committees and French and European guidelines for animal care. Experimental meningococcal infections were induced by the intraperitoneal injection of *N. meningitidis* MC58, with 2.5 mg of human transferrin per mouse as a source of iron (Sigma-Aldrich). When genetically modified animals were used, litters were studied as controls, as indicated. Anti-NK1.1 mAb treatment (100 μg per mouse; PK136, BioXCell) was administered intraperitoneally 1 day before Nm infection. Anti-aGM1 mAb treatment (50 μg per mouse; BioLegend) was administered intraperitoneally 2 days before Nm infection. Survival was scored. Bacterial load in the blood was also evaluated by plating serial dilutions on GCB medium (Difco) supplemented with Kellogg's supplements and VCF (Bio-Rad), and the results are expressed as the number of colony-forming units (CFU) per milliliter. For CFP treatment, 100 μg of endotoxin-free HIS-tagged MoCFP was administered 6 hours before infection (35). No blinding or randomization was performed.

Nm opsonization

Nm (5×10^7) were incubated at 37°C for 30 min in PBS, CaCl2, and Mg plus 20% of human serum or CFP-depleted serum (Complement Technology Inc.). Bacteria were then incubated with NCR-Fc (20 μg/ml) precomplexed with F(ab′)2 anti-human Fc (Jackson Laboratory) at 37°C for 30 min. Bacteria are then washed and fixed with 3% paraformaldehyde.

Statistical analyses

Details of statistical analysis for each experiment are given in the relevant figure legend and in raw data table. Normality and variance were verified. *t* tests, Mann-Whitney tests, and one- and two-way ANOVAs were performed using Prism 7 (GraphPad Software). Kaplan-Meier curves were used to analyze mouse survival. Significance was calculated as Nm dose stratified with the help of a CIML statistician. Statistical significance was assumed if the *P* value was <0.05 for a tested difference. *P* values are indicated in the figures.

Supplementary Material

Refer to Web version on PubMed Central for supplementary material.

Acknowledgments

We thank the laboratories of E.V. and M.-K.T. and Innate Pharma for help and discussions. We thank the CIML (mouse house and core cytometry), the Ciphe (BSL-3), and the Pasteur Institute facilities. We thank M. Pophillat for the help in proteomic analyses; M. Pierres and A. Bole for help in the generation of anti-B12 cell hybridomas; S. Carpentier (MI-mAbs) for biostatistics; C. Cognet, P. Kruse, and M. Bléry for their collaboration; and the CIML bioinformatics platform for analyses. S. Jonjic (University of Rijeka) provided the B12 cells. A. Moretta (University of Genoa) provided the anti-HuNKp46 BAB281 mAb hybridoma. W. Song (University of Pennsylvania) provided the anti-MoCFP pAbs. O. Mandelboim (University of Jerusalem) provided the *NCR1GFP/GFP* mice.

Funding: This work was supported by a European Research Council advanced grant (T.I.L.C. to E.V.); Agence Nationale de la Recherche (to E.V. and M.-K.T.); Equipe Labellisée “La Ligue,” Ligue Nationale contre le Cancer (to E.V.); and institutional grants to the CIML (INSERM, CNRS, and Aix-Marseille University), to Marseille Immunopôle, and to the Pasteur Institute.

References and notes

1. Artis D, Spits H. The biology of innate lymphoid cells. Nature. 2015; 517:293–301. [PubMed: 25592534]
2. Eberl G, Colonna M, Di Santo JP, McKenzie ANJ. Innate lymphoid cells. Innate lymphoid cells: A new paradigm in immunology. Science. 2015; 348:aaa6566. [PubMed: 25999512]
3. Vivier E, Raulet DH, Moretta A, Caligiuri MA, Zitvogel L, Lanier LL, Yokoyama WM, Ugolini S. Innate or adaptive immunity? The example of natural killer cells. Science. 2011; 331:44–49. [PubMed: 21212348]
4. Vivier E, Nunès JA, Vély F. Natural killer cell signaling pathways. Science. 2004; 306:1517–1519. [PubMed: 15567854]
5. Long EO, Kim HS, Liu D, Peterson ME, Rajagopalan S. Controlling natural killer cell responses: Integration of signals for activation and inhibition. Annu Rev Immunol. 2013; 31:227–258. [PubMed: 23516982]
6. Yokoyama WM, Kim S. Licensing of natural killer cells by self-major histocompatibility complex class I. Immunol Rev. 2006; 214:143–154. [PubMed: 17100882]
7. Brodin P, Kärre K, Höglund P. NK cell education: Not an on-off switch but a tunable rheostat. Trends Immunol. 2009; 30:143–149. [PubMed: 19282243]
8. Shifrin N, Raulet DH, Ardolino M. NK cell self tolerance, responsiveness and missing self recognition. Semin Immunol. 2014; 26:138–144. [PubMed: 24629893]
9. Lanier LL. Up on the tightrope: Natural killer cell activation and inhibition. Nat Immunol. 2008; 9:495–502. [PubMed: 18425106]
10. Wu N, Veillette A. SLAM family receptors in normal immunity and immune pathologies. Curr Opin Immunol. 2016; 38:45–51. [PubMed: 26682762]
11. Moretta L, Bottino C, Pende D, Castriconi R, Mingari MC, Moretta A. Surface NK receptors and their ligands on tumor cells. Semin Immunol. 2006; 18:151–158. [PubMed: 16730454]
12. Diefenbach A, Colonna M, Koyasu S. Development, differentiation, and diversity of innate lymphoid cells. Immunity. 2014; 41:354–365. [PubMed: 25238093]
13. Spits H, Artis D, Colonna M, Diefenbach A, Di Santo JP, Eberl G, Koyasu S, Locksley RM, McKenzie AN, Mebius RE, Powrie F, et al. Innate lymphoid cell—A proposal for uniform nomenclature. Nat Rev Immunol. 2013; 13:145–149. [PubMed: 23348417]
14. Yu J, Mitsui T, Wei M, Mao H, Butchar JP, Shah MV, Zhang J, Mishra A, Alvarez-Breckenridge C, Liu X, Liu S, et al. NKp46 identifies an NKT cell subset susceptible to leukemic transformation in mouse and human. J Clin Invest. 2011; 121:1456–1470. [PubMed: 21364281]
15. Raulet DH, Gasser S, Gowen BG, Deng W, Jung H. Regulation of ligands for the NKG2D activating receptor. Annu Rev Immunol. 2013; 31:413–441. [PubMed: 23298206]
16. Kruse PH, Matta J, Ugolini S, Vivier E. Natural cytotoxicity receptors and their ligands. Immunol Cell Biol. 2014; 92:221–229. [PubMed: 24366519]

Europe PMC Funders Author Manuscripts

17. Mandelboim O, Lieberman N, Lev M, Paul L, Arnon TI, Bushkin Y, Davis DM, Strominger JL, Yewdell JW, Porgador A. Recognition of haemagglutinins on virus-infected cells by NKp46 activates lysis by human NK cells. Nature. 2001; 409:1055–1060. [PubMed: 11234016]
18. Chaushu S, Wilensky A, Gur C, Shapira L, Elboim M, Halftek G, Polak D, Achdout H, Bachrach G, Mandelboim O. Direct recognition of *Fusobacterium nucleatum* by the NK cell natural cytotoxicity receptor NKp46 aggravates periodontal disease. PLOS Pathog. 2012; 8:e1002601. [PubMed: 22457623]
19. Vitenshtein A, Charpak-Amikam Y, Yamin R, Bauman Y, Isaacson B, Stein N, Berhani O, Dassa L, Gamliel M, Gur C, Glasner A, et al. NK cell recognition of *Candida glabrata* through binding of NKp46 and NCR1 to fungal ligands Epa1, Epa6, and Epa7. Cell Host Microbe. 2016; 20:527–534. [PubMed: 27736647]
20. Brandt CS, Baratin M, Yi EC, Kennedy J, Gao Z, Fox B, Haldeman B, Ostrander CD, Kaifu T, Chabannon C, Moretta A, et al. The B7 family member B7-H6 is a tumor cell ligand for the activating natural killer cell receptor NKp30 in humans. J Exp Med. 2009; 206:1495–1503. [PubMed: 19528259]
21. Bloushtain N, Qimron U, Bar-Ilan A, Hershkovitz O, Gazit R, Fima E, Korc M, Vlodavsky I, Bovin NV, Porgador A. Membrane-associated heparan sulfate proteoglycans are involved in the recognition of cellular targets by NKp30 and NKp46. J Immunol. 2004; 173:2392–2401. [PubMed: 15294952]
22. Hecht M-L, Rosental B, Horlacher T, Hershkovitz O, De Paz JL, Noti C, Schauer S, Porgador A, Seeberger PH. Natural cytotoxicity receptors NKp30, NKp44 and NKp46 bind to different heparan sulfate/heparin sequences. J Proteome Res. 2009; 8:712–720. [PubMed: 19196184]
23. Hershkovitz O, Jarahian M, Zilka A, Bar-Ilan A, Landau G, Jivov S, Tekoah Y, Glicklis R, Gallagher JT, Hoffmann SC, Zer H, et al. Altered glycosylation of recombinant NKp30 hampers binding to heparan sulfate: A lesson for the use of recombinant immunoreceptors as an immunological tool. Glycobiology. 2008; 18:28–41. [PubMed: 18006589]
24. Baychelier F, Sennepin A, Ermonval M, Dorgham K, Debré P, Vieillard V. Identification of a cellular ligand for the natural cytotoxicity receptor NKp44. Blood. 2013; 122:2935–2942. [PubMed: 23958951]
25. Garg A, Barnes PF, Porgador A, Roy S, Wu S, Nanda JS, Griffith DE, Girard WM, Rawal N, Shetty S, Vankayalapati R. Vimentin expressed on *Mycobacterium tuberculosis* infected human monocytes is involved in binding to the NKp46 receptor. J Immunol. 2006; 177:6192–6198. [PubMed: 17056548]
26. Gur C, Porgador A, Elboim M, Gazit R, Mizrahi S, Stern-Ginossar N, Achdout H, Ghadially H, Dor Y, Nir T, Doviner V, et al. The activating receptor NKp46 is essential for the development of type 1 diabetes. Nat Immunol. 2010; 11:121–128. [PubMed: 20023661]
27. Blatt AZ, Pathan S, Ferreira VP. Properdin: A tightly regulated critical inflammatory modulator. Immunol Rev. 2016; 274:172–190. [PubMed: 27782331]
28. Moretta A, Bottino C, Vitale M, Pende D, Cantoni C, Mingari MC, Biassoni R, Moretta L. Activating receptors and coreceptors involved in human natural killer cell-mediated cytolysis. Annu Rev Immunol. 2001; 19:197–223. [PubMed: 11244035]
29. Ram S, Lewis LA, Rice PA. Infections of people with complement deficiencies and patients who have undergone splenectomy. Clin Microbiol. Rev. 2010; 23:740–780. [PubMed: 20930072]
30. Coureuil M, Join-Lambert O, Lécuyer H, Bourdoulous S, Marullo S, Nassif X. Pathogenesis of meningococcemia. Cold Spring Harb Perspect Med. 2013; 3:a012393. [PubMed: 23732856]
31. Bosis S, Mayer A, Esposito S. Meningococcal disease in childhood: Epidemiology, clinical features and prevention. J Prev Med Hyg. 2015; 56:E121–E124. [PubMed: 26788732]
32. Kugelberg E, Gollan B, Tang CM. Mechanisms in *Neisseria meningitidis* for resistance against complement-mediated killing. Vaccine. 2008; 26(suppl. 8):I34–I39. [PubMed: 19388162]
33. Deauvieau F, Fenis A, Dalençon F, Burdin N, Vivier E, Kerdiles Y. Lessons from NK cell deficiencies in the mouse. Curr Top Microbiol Immunol. 2016; 395:173–190. [PubMed: 26385768]

34. Victorino F, Sojka DK, Brodsky KS, McNamee EN, Masterson JC, Homann D, Yokoyama WM, Eltzschig HK, Clambey ET. Tissue-resident NK cells mediate ischemic kidney injury and are not depleted by anti–asialo-GM1 antibody. J Immunol. 2015; 195:4973–4985. [PubMed: 26453755]
35. Ali YM, Hayat A, Saeed BM, Haleem KS, Alshamrani S, Kenawy HI, Ferreira VP, Saggu G, Buchberger A, Lachmann PJ, Sim RB, et al. Low-dose recombinant properdin provides substantial protection against *Streptococcus pneumoniae* and *Neisseria meningitidis* infection. Proc Natl Acad Sci USA. 2014; 111:5301–5306. [PubMed: 24706855]
36. Ross SC, Densen P. Complement deficiency states and infection: Epidemiology, pathogenesis and consequences of neisserial and other infections in an immune deficiency. Medicine. 1984; 63:243–273. [PubMed: 6433145]
37. Pessino A, Sivori S, Bottino C, Malaspina A, Morelli L, Moretta L, Biassoni R, Moretta A. Molecular cloning of NKp46: A novel member of the immunoglobulin superfamily involved in triggering of natural cytotoxicity. J Exp Med. 1998; 188:953–960. [PubMed: 9730896]
38. Crozat K, Guiton R, Contreras V, Feuillet V, Dutertre C-A, Ventre E, Manh T-PV, Baranek T, Storset AK, Marvel J, Boudinot P, et al. The XC chemokine receptor 1 is a conserved selective marker of mammalian cells homologous to mouse CD8α+ dendritic cells. J Exp Med. 2010; 207:1283–1292. [PubMed: 20479118]
39. Nevins AM, Subramanian A, Tapia JL, Delgado DP, Tyler RC, Jensen DR, Ouellette AJ, Volkman BF. A requirement for metamorphic interconversion in the antimicrobial activity of chemokine XCL1. Biochemistry. 2016; 55:3784–3793. [PubMed: 27305837]
40. Yang D, Chen Q, Hoover DM, Staley P, Tucker KD, Lubkowski J, Oppenheim JJ. Many chemokines including CCL20/MIP-3α display antimicrobial activity. J Leukoc. Biol. 2003; 74:448–455. [PubMed: 12949249]
41. Bryceson YT, March ME, Ljunggren H-G, Long EO. Synergy among receptors on resting NK cells for the activation of natural cytotoxicity and cytokine secretion. Blood. 2006; 107:159–166. [PubMed: 16150947]
42. Rosadini CV, Kagan JC. Early innate immune responses to bacterial LPS. Curr Opin Immunol. 2017; 44:14–19.
43. Pazina T, Shemesh A, Brusilovsky M, Porgador A, Campbell KS. Regulation of the functions of natural cytotoxicity receptors by interactions with diverse ligands and alterations in splice variant expression. Front Immunol. 2017; 8:369. [PubMed: 28424697]
44. Zaferani A, Vivès RR, van der Pol P, Navis GJ, Daha MR, van Kooten C, Lortat-Jacob H, Seelen MA, van den Born J. Factor h and properdin recognize different epitopes on renal tubular epithelial heparan sulfate. J Biol Chem. 2012; 287:31471–31481. [PubMed: 22815489]
45. Marcenaro E, Augugliaro R, Falco M, Castriconi R, Parolini S, Sivori S, Romeo E, Millo R, Moretta L, Bottino C, Moretta A. CD59 is physically and functionally associated with natural cytotoxicity receptors and activates human NK cell-mediated cytotoxicity. Eur J Immunol. 2003; 33:3367–3376. [PubMed: 14635045]
46. Kemper C, Atkinson JP, Hourcade DE. Properdin: Emerging roles of a patternrecognition molecule. Annu Rev Immunol. 2010; 28:131–155. [PubMed: 19947883]
47. Ebbo M, Gérard L, Carpentier S, Vély F, Cypowyj S, Farnarier C, Vince N, Malphettes M, Fieschi C, Oksenhendler E, Schleinitz N, et al. Low circulating natural killer cell counts are associated with severe disease in patients with common variable immunodeficiency. EBioMedicine. 2016; 6:222–230. [PubMed: 27211564]
48. Schleinitz N, Cognet C, Guia S, Laugier-Anfossi F, Baratin M, Pouget J, Pelissier J-F, Harle J-R, Vivier E, Figarella-Branger D. Expression of the CD85j (leukocyte Ig-like receptor 1, Ig-like transcript 2) receptor for class I major histocompatibility complex molecules in idiopathic inflammatory myopathies. Arthritis Rheum. 2008; 58:3216–3223. [PubMed: 18821690]
49. Dennler P, Chiotellis A, Fischer E, Brégeon D, Belmant C, Gauthier L, Lhospice F, Romagne F, Schibli R. Transglutaminase-based chemo-enzymatic conjugation approach yields homogeneous antibody–drug conjugates. Bioconjug Chem. 2014; 25:569–578. [PubMed: 24483299]

Europe PMC Funders Author Manuscripts

Editor's summary

Inter-Innate Cooperation

The different branches of the immune system work together like a well-oiled machine, but how this coordination occurs is less well understood. Narni-Mancinelli *et al.* have found one such mechanism—cross-talk between the alternative complement pathway and natural killer (NK) cells and innate lymphoid cells (ILCs). They report that complement factor P (CFP), a positive regulator of the alternative complement pathway, binds NKp46, which is expressed on subsets of NK cells and ILC1 and ILC3. Patients lacking CFP are more susceptible to *Neisseria meningitidis* infection, and in mice this CFP protection was dependent on NKp46 and group 1 ILCs. These data suggest ILCs and the alternative complement pathway cooperate to fight off bacterial infection.

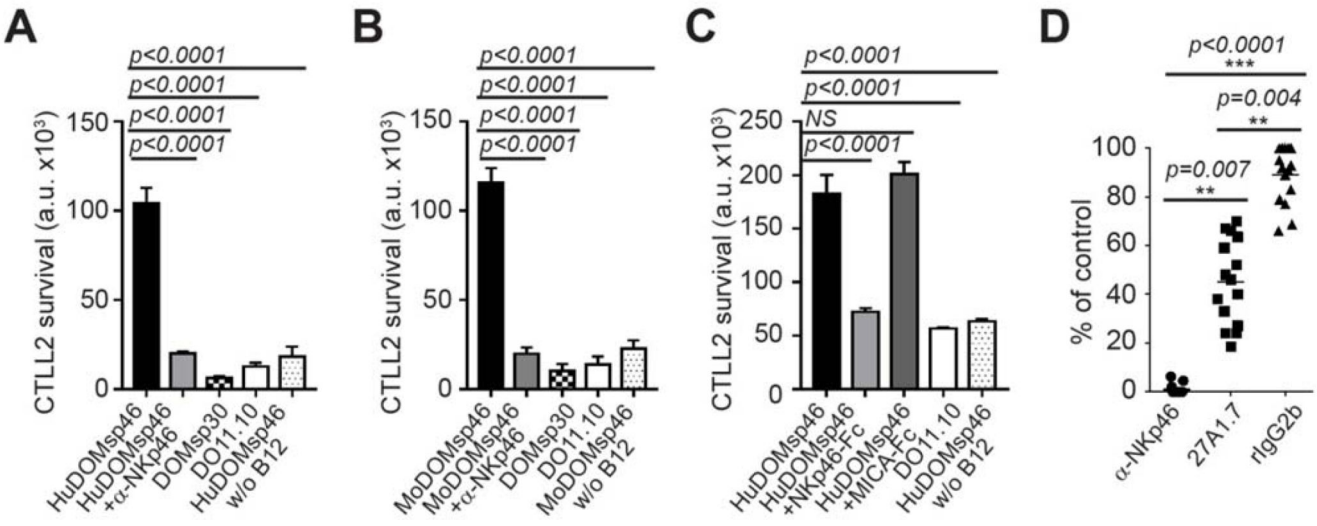

Fig. 1. B12 cells express a ligand for NKp46.

Reporter cells were cocultured with B12 cells in the presence of the indicated anti-HuNKp46 (BAB281) (**A**) or anti-MoNKp46 (29A1.4) mAbs (**B**) or with soluble recombinant Fc fusion proteins (**C**). a.u., arbitrary units; ns, not significant. Cell activation was assessed by evaluating IL-2 levels in the coculture supernatant in a standard CTLL-2 survival assay. (**D**) HuDOMsp46 reporter cells were cocultured with B12 cells in the presence of anti-HuNKp46 mAb (BAB281), the 27A1.7 mAb generated against B12 cells, or its corresponding isotype control (rIgG2b). Data are means of triplicates ± SD and are the pooled results of two (A to C) or four (D) independent experiments. (A to C) Two-way ANOVA, with Bonferroni correction for multiple comparisons, $n = 5$. (D) Kruskal-Wallis test, with Dunn's test for multiple comparisons, $n = 15$.

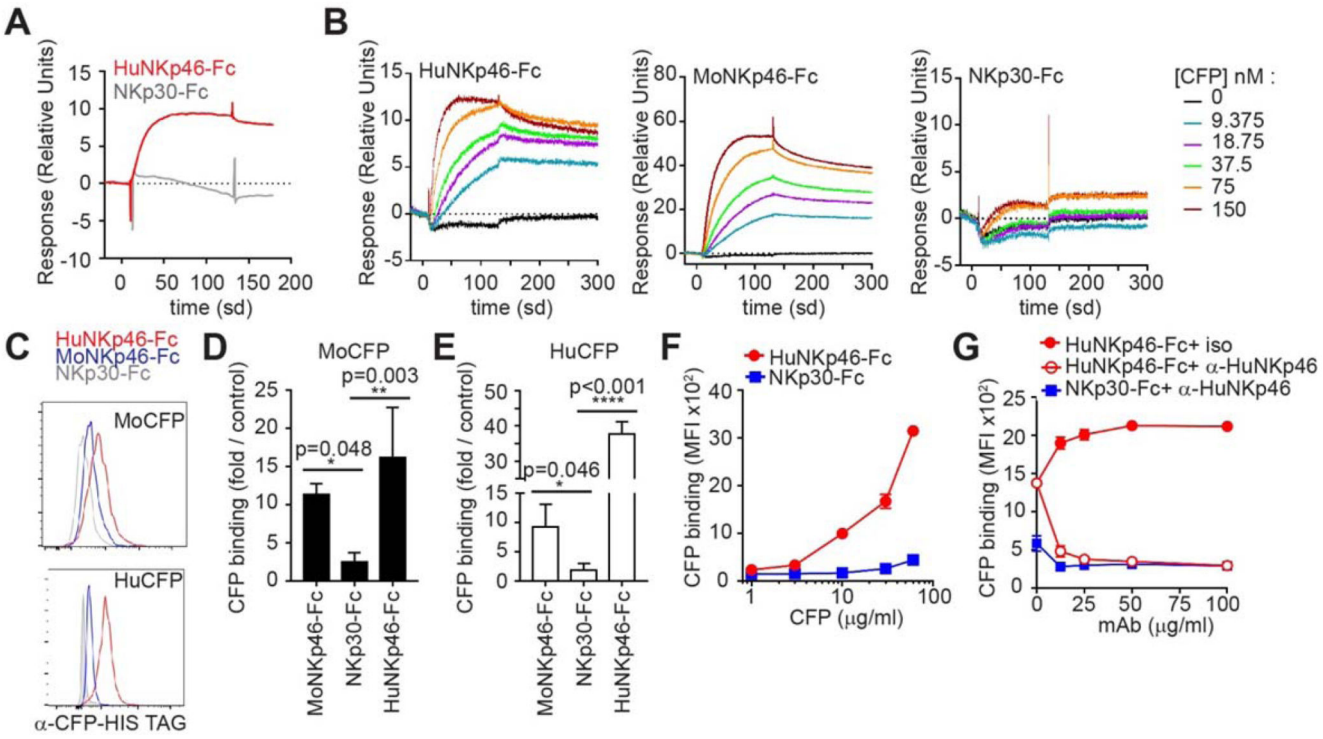

Fig. 2. CFP binds to NKp46.

Flow sensorgrams of the indicated NCR-Fc constructs with 10 nM CFP purified from human serum (**A**) or at the indicated concentrations of soluble recombinant HuCFP-HIS (**B**) flowing over a flow cell with similar immobilized NCR-Fc response units. (**C**) Cytometric profiles showing the binding of recombinant HIS-tagged CFP to beads coated with the indicated NCR-Fc molecules. (**D** and **E**) Binding is expressed as a fold increase in mean fluorescence intensity (MFI) over the control without CFP ± SD. $n = 3$ to 4, one-way ANOVA, Bonferroni correction for multiple comparisons. The experiment was performed with a range of CFP concentrations (**F**) and in the presence of anti-NKp46 mAb (BAB281) or isotype control mAb (**G**). The data presented are the pooled results of three independent experiments in (D) and (E) and two in (F) and (G).

Europe PMC Funders Author Manuscripts

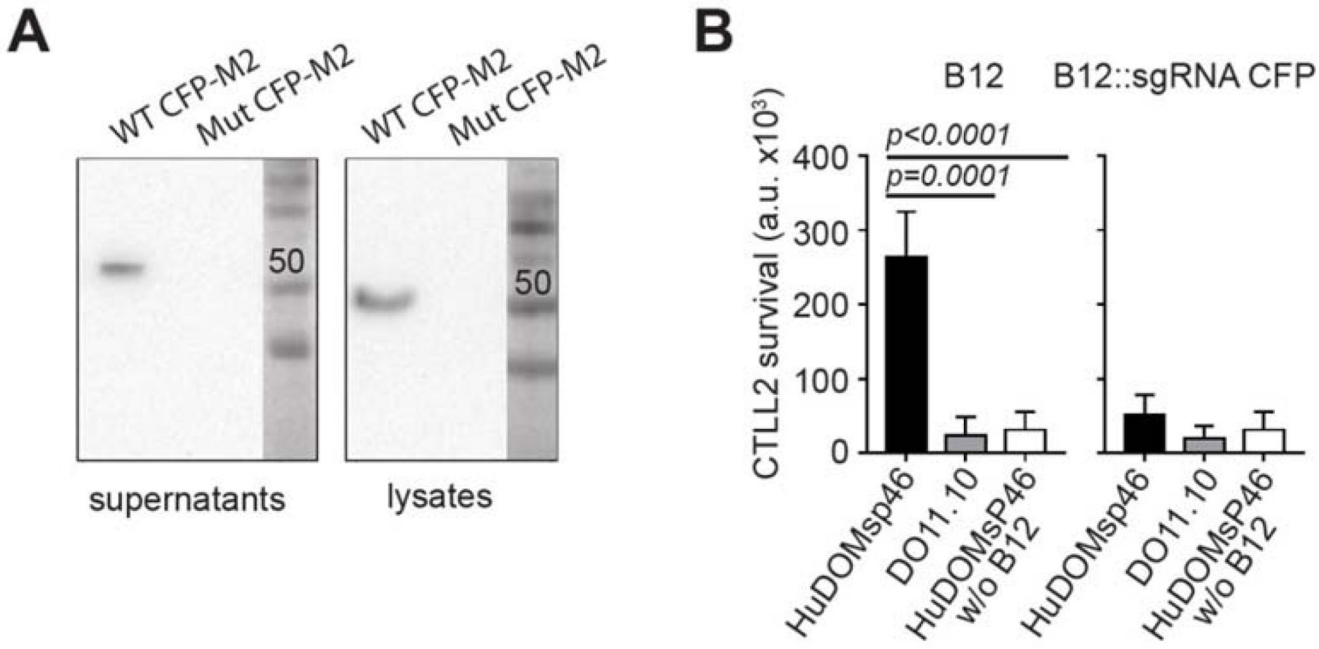

Fig. 3. *Cfp* silencing in B12 cells impaired NKp46 reporter cell activation.

Cfp silencing was achieved with the CRISPR/Cas9 system. (**A**) WT and Cfp mutated cDNA were inserted, in frame with a M2 TAG, into an expression vector, which was then used to transfect 293T cells. Protein levels were analyzed by Western blotting of the supernatant and cell lysate for M2. (**B**) Reporter cells were cocultured with the indicated control or with *Cfp*-silenced B12 cells. Cell activation was assessed by evaluating IL-2 levels in the coculture supernatant in a standard CTLL-2 survival assay. Data are means of triplicates ± SD and are the pooled results of three independent experiments. One-way ANOVA, with Bonferroni correction for multiple comparisons, $n = 8$ to 9.

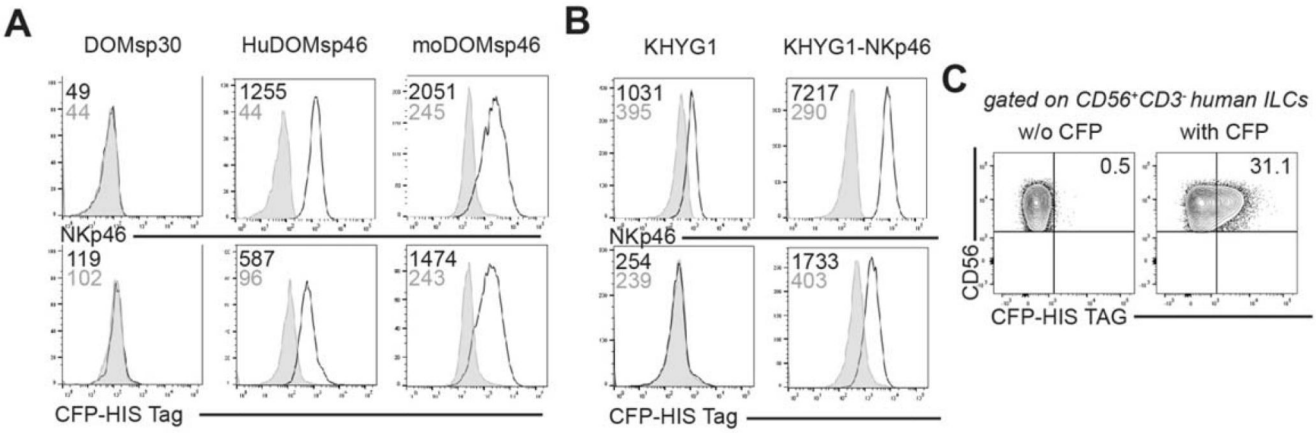

Fig. 4. CFP binds on NKp46^{+}-expressing cells.

(**A** and **B**) Binding of soluble recombinant HIS-tagged HuCFP to the cells indicated (see Materials and Methods). Numbers indicate the MFI. (**C**) CFP binding to primary human IL-2–activated bulk NK cells. Numbers in quadrants indicate frequencies. Data are representative of three independent experiments in (A) and (B) and two independent experiments in (C).

Europe PMC Funders Author Manuscripts

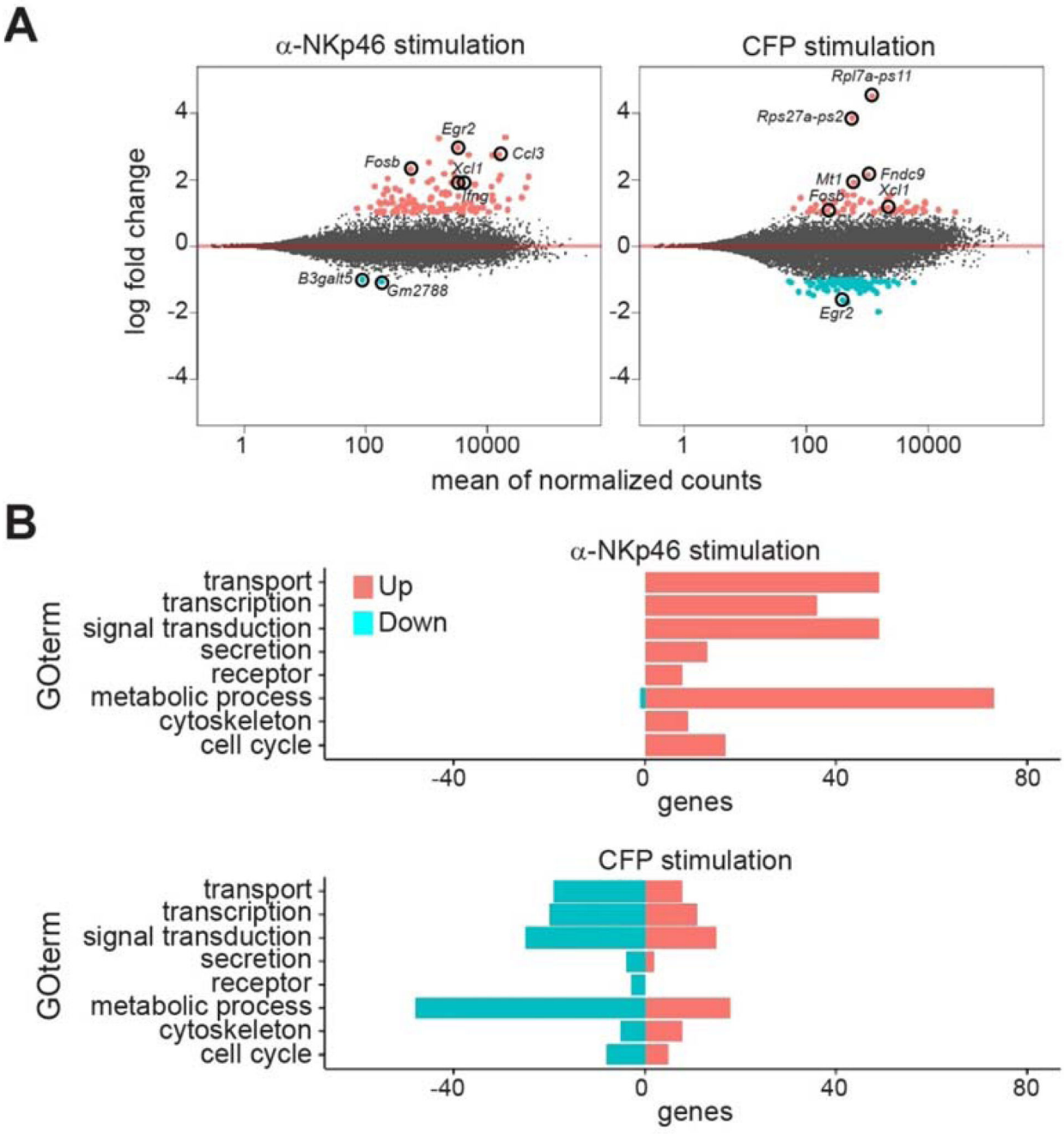

Fig. 5. CFP and anti-NKp46 mAbs induce distinct genetic programs in NK cells.

Flow cytometry–sorted NK cells from C57BL/6 mice were stimulated for 4 hours with MoCFP-HIS precomplexed with an anti-HIS tag antibody–coated plates or with anti-NKp46 mAbs or isotype mAbs. We then extracted and sequenced mRNA from the cells. (**A**) Scatterplot of differential expression analyzed by DESeq2. Genes displaying significantly higher (pink) or lower (blue) levels of expression after stimulation with anti-NKp46 mAb or CFP stimulation than after incubation with the isotype control are displayed. The log2 fold change for each gene is shown in the *y* axis, and the total number of counts recorded for the

Europe PMC Funders Author Manuscripts

gene is shown in the *x* axis. (**B**) Gene Ontology (GO) terms associated with differentially expressed genes are shown.

Europe PMC Funders Author Manuscripts

Europe PMC Funders Author Manuscripts

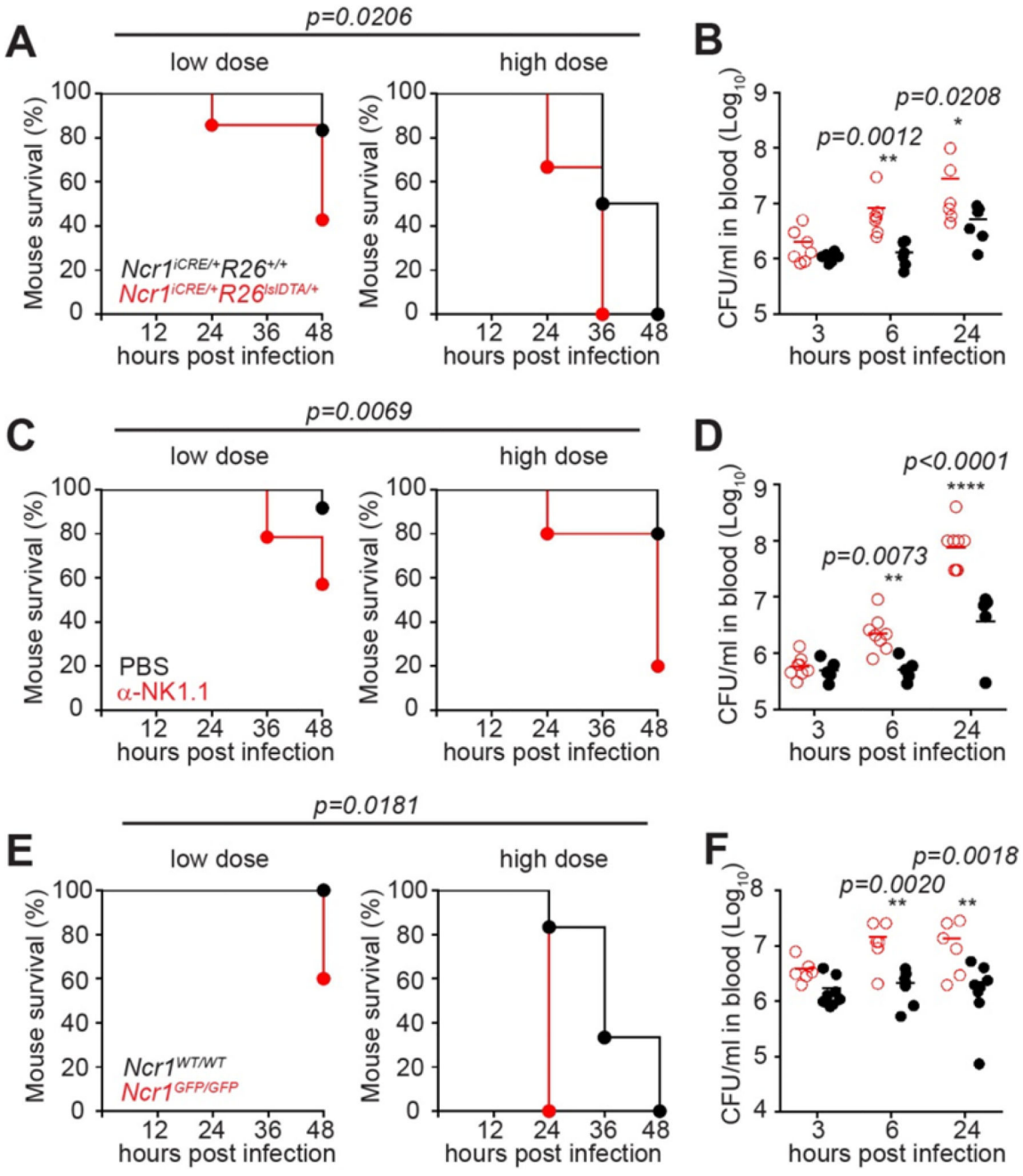

Fig. 6. NKp46^{+} ILCs and NKp46 are involved in the control of Nm infection.

Geneti cally engineered NKp46^{+} cell–deficient mice (*Ncr1*$^{iCRE/+}$*R26*$^{lslDTA/+}$) and control littermates (**A** and **B**), WT control mice with and without anti-NK1.1 mAb treatment (**C** and **D**), and *Ncr1*$^{GFP/GFP}$ and control littermates (**E** and **F**) were infected intraperitoneally with 2 × 10^{6} (low dose) or 5.6 × 10^{6} to 8 × 10^{6} (high dose) Nm. Survival after treatment with the indicated dose (A, C, and E) and bacterial load after infection with 2 × 10^{6} bacteria (B, D, and F) were monitored over time. Dose-stratified log-rank tests were performed to analyze survival: n = 16 (A), n = 17 to 19 (C), and n = 29 (E). Bacterial load shown in (B), (D), and

(F) is representative of two experiments. Two-way ANOVA with Bonferroni correction for multiple tests with $n = 6$ in (B), $n = 5$ to 8 in (D), and $n = 6$ to 8 in (E).

Europe PMC Funders Author Manuscripts

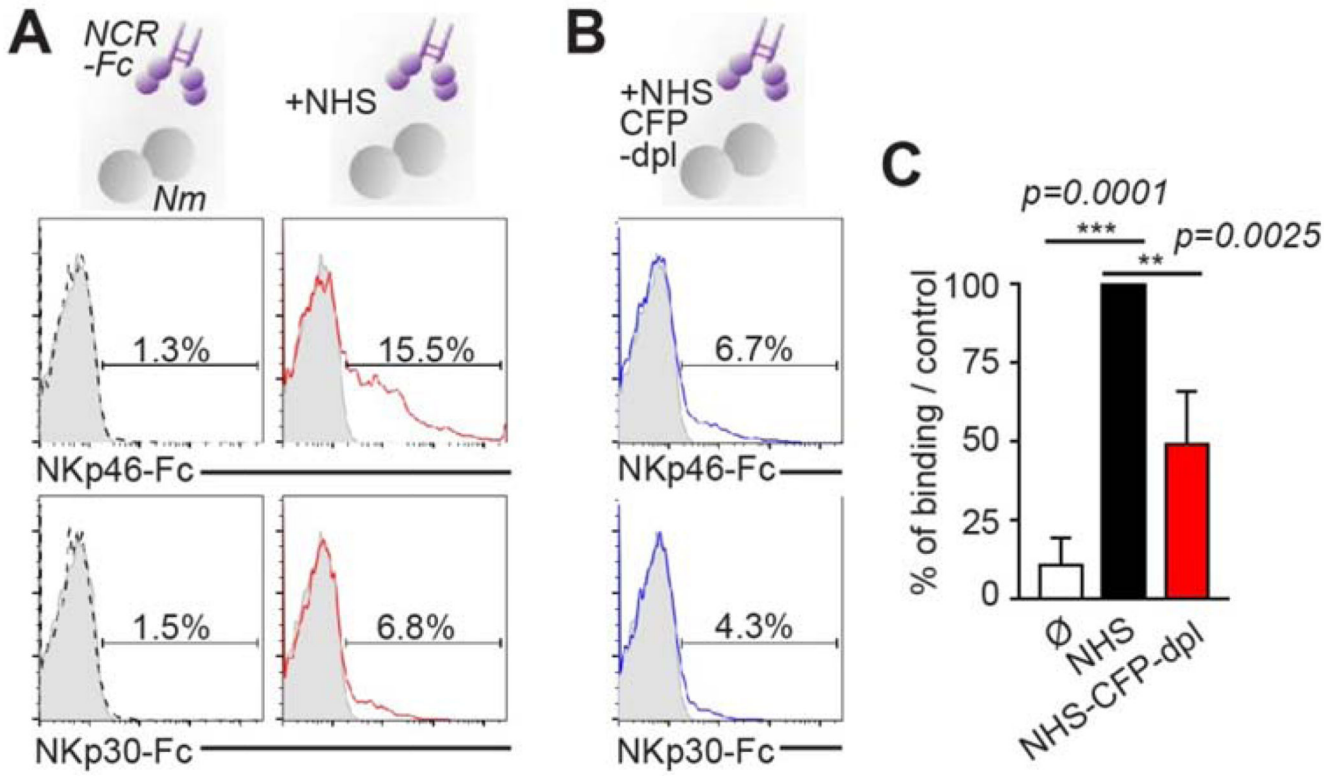

Fig. 7. NKp46 binds to serum-opsonized Nm bacteria.

(**A** and **B**) Representative cytometric profiles of NCR-Fc staining on Nm bacteria in the conditions indicated. Gray solid histogram: Nm bacteria only. (**C**) Data are presented as a percentage of NHS control binding. The data presented are the pooled results of three independent experiments. One-way ANOVA with Bonferroni correction for multiple comparisons.

Europe PMC Funders Author Manuscripts

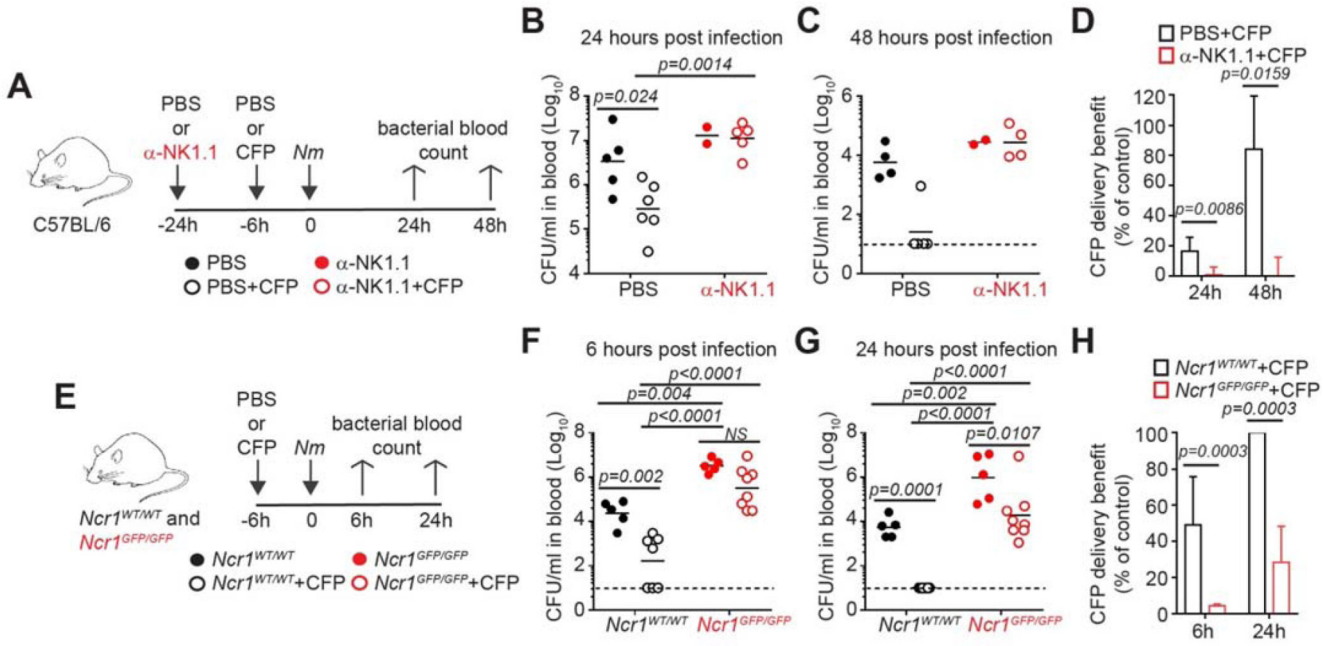

Fig. 8. NKp46^{+} ILCs and NKp46 contribute to the therapeutic benefits of CFP delivery on bacteremia during Nm infection.

(**A** to **D**) WT mice were treated as shown in (A). Bacterial load after 24 hours (B) and 48 hours (C) of infection with 1×10^7 Nm. One-way ANOVA with Bonferroni correction for multiple tests, $n = 6$. (D) Representation of the CFP benefit observed in (B) and (C) for each CFP-treated group, expressed as the percentage decrease in bacterial load observed for each mouse treated with CFP relative to the mean value for untreated individuals ± SD. Representative of two independent experiments. Unpaired *t* test at 24 hours and Mann-Whitney test at 48 hours. (**F** and **G**) *Ncr1*$^{WT/WT}$ and *Ncr1*$^{GFP/GFP}$ littermates were treated as shown in (**E**). Bacterial load after 6 hours (F) and 24 hours (G) of infection with 2×10^6 Nm. $n = 5$ to 8, representative of two independent experiments; two-way ANOVA with Tukey's correction for multiple tests. (**H**) Representation of the CFP benefit observed in (F) and (G), as calculated in (D); Mann-Whitney test at 6 and 24 hours.

Europe PMC Funders Author Manuscripts